Barkhan (Balochistan) earthquakes of June 26 and July 12, 1999: Source parameters from teleseismic body waves

Tariq Mahmood[1], Karam Khan[1], Talat Iqbal[1], Muhammad Qaisar[2] and Suhail Ahmed[1]
[1]Micro Seismic Study Programme P. O. Box 3339, Islamabad
[2]Center for Earthquake Studies, National Centre for Physics, Quaid-i-Azam University Campus, Islamabad

Abstract

Two moderate earthquakes occurred on June 26 and July 12, 1999 at Barkhan, in at the northern limb of the Sibbi Syntaxis occupied by the southern Sulaiman Ranges. Source characteristics of these earthquakes were studied using the teleseismic body waves recorded at the IRIS Global Seismographic Network. The P and SH waveforms of these events were inverted to double couple source using the method of Kikuchi and Kanamori (1991). The azimuthal coverage of seismograph stations is good enough to resolve some details of heterogeneous moment tensor. Orientation and length of the fault are derived from aftershocks related with this earthquake event. The data show that the slip on the northeastern sections of the Karmari and Barkhan thrusts was responsible for these earthquakes. The focal mechanism solutions suggest thrust faulting. The strike, dip and rake of the causative fault of the June 26 earthquake are respectively 243°, 39° and 92° and that of July 12, earthquake are 237°, of 32°, and 111°. The seismic moment is estimated as $M_o = 2.3 \times 10^{17}$ Nm for June 26 and $M_o = 3.3 \times 10^{17}$ Nm for July 12, 1999.

Keywords: Barkhan; Earthquake; Sulaiman ranges; Source parameters; Teleseismic body waves; Focal mechanism solutions; Seismic moment

1. Introduction

On the early morning of June 26, 1999 a moderate earthquake of magnitude (m_b) 5.5 occurred in a mountaneous and sparsely populated region of Balochistan. The epicenter was located at 29.97°N and 69.77°E in the southern Sulaiman Range near the town of Barkhan about 100 km west of the city of Dera Ghazi Khan (Fig. 1). The Sulaiman Ranges make a major south-directed fold at their southern end north of the Quetta-Sibi syntax (also termed Sibi Trough). Together with Kirthar Ranges in the south, these ranges define a transpressional thrust-fold belt along the western left-lateral strike-slip boundary of the Indian subcontinent (Abdul-Gawad, 1971; Sarwar and DeJong, 1979; Lawrence et al., 1981). Figs. 1-2 show the main thrust faults in the region named as Pirkoh thrust, Karmari thrust, Karahi thrust, Chinjan thrust and Zhob valley thrust (Bender and Raza, 1995).

The Barkhan main shock (June 26, 1999) was followed by 35 aftershocks of magnitude ≥2.0 within four days of its occurrence. The largest aftershock of June 30, 1999 having magnitude 5.0 occurred almost at the same location as the main shock (Fig. 3). Hypocentral locations of the aftershocks were determined with the help of computer code HYPO71PC (Lee, 1990) using body wave data recorded by local seismic network. The spatial distribution of the well-located aftershocks forms a cluster just NE of the main shock (Fig. 3).

On July 12, 1999 the region was rocked again by another earthquake of magnitude m_b = 5.5 that occurred on almost the same location at 29.92°N and 69.54°E (Fig. 2). This earthquake was followed by about 30 aftershocks of magnitude ≥2.0 upto July 31. The largest being of magnitude 5.0 that occurred on July 28, 1999. The spatial distribution of the well-located aftershocks forms a cluster just NE of the main shock (Fig. 4).
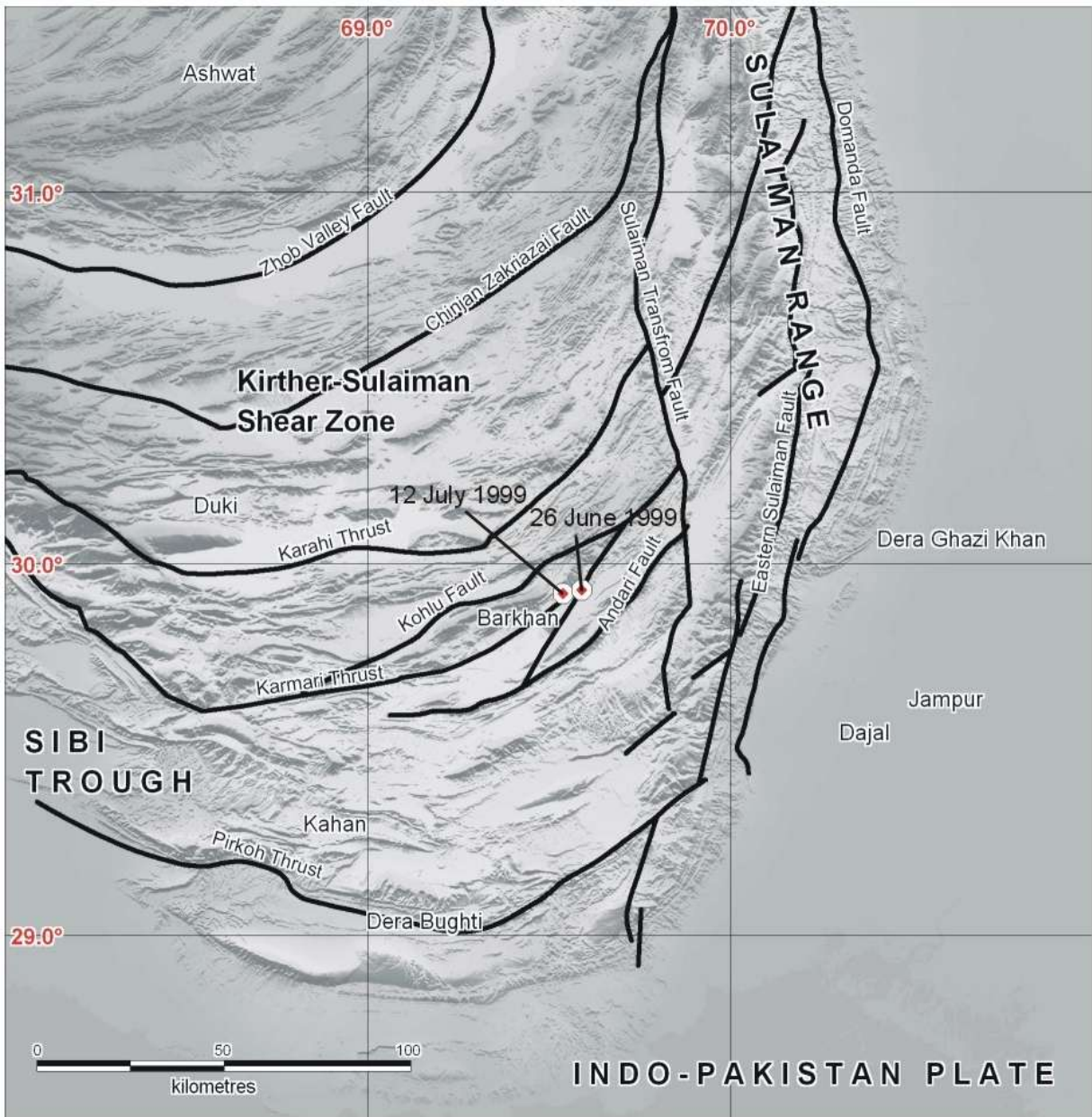
Fig. 1. Map showing the epicentral locations of the earthquakes of June 26 and July 12, 1999 in context of major tectonic structures of the area (after Bannert et. al., 1992).
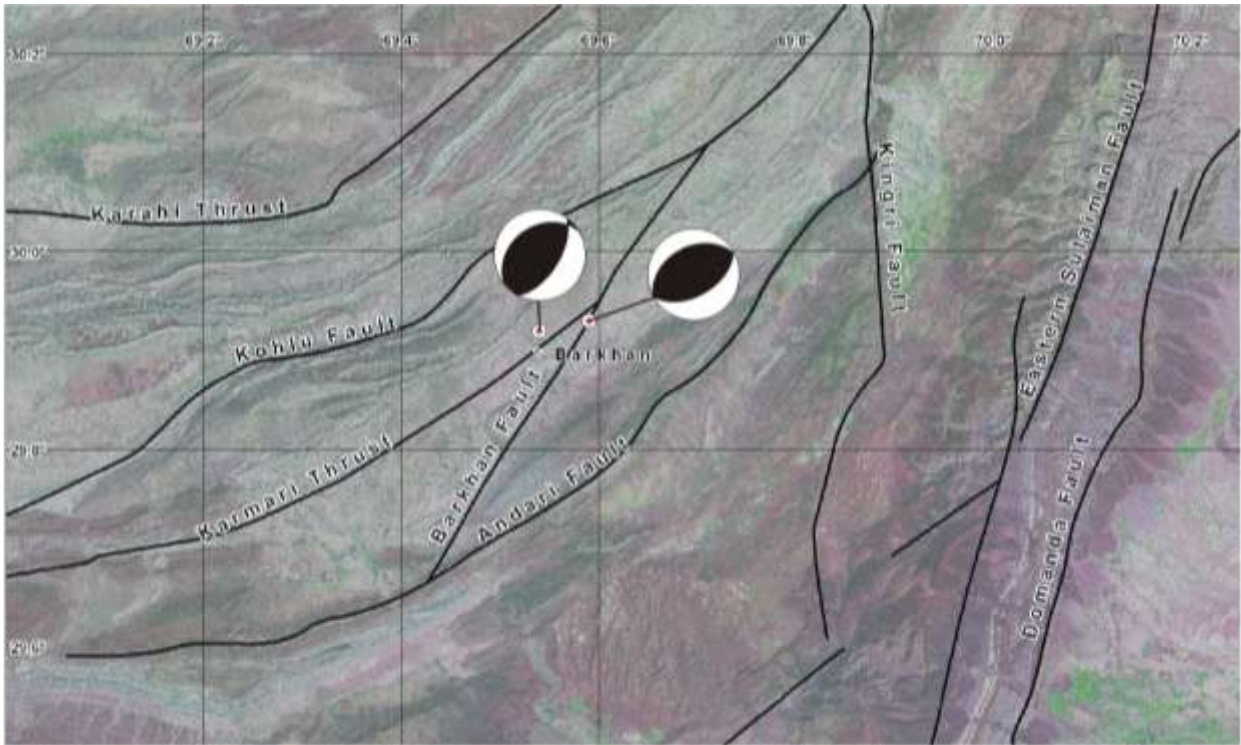
Fig. 2. Map showing the epicentral locations and focal mechanism solutions of the earthquakes of June 26 and July 12, 1999 in context of local tectonics of the area (after Bannert et. al., 1992).
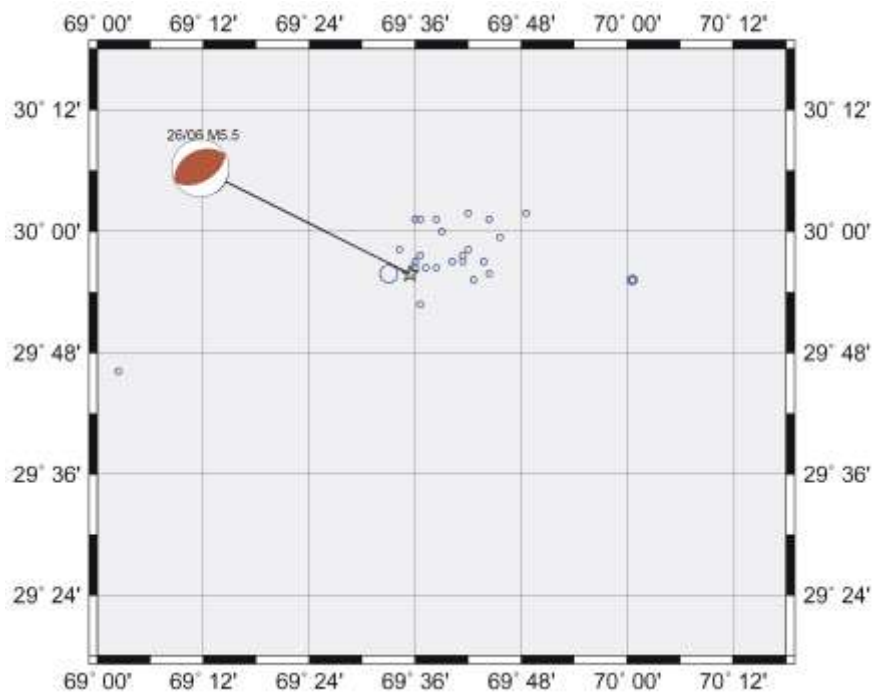

Fig. 3. Map showing the epicentral location of the Barkhan earthquake of June 26, 1999 and distribution of aftershocks (MSSP Data).

The main purpose of this study is to determine the mechanism of these events including fault geometry, fault area, seismic moment and other related source parameters, using waveform inversion. Determination of these parameters is useful not only for understanding the physics of earthquakes but also for estimating the potential hazard associated with stress changes in the faults adjacent to the earthquake area.

2. Body wave analysis

The teleseismic broadband data set used in this study was retrieved from Data Management Centre of the Incorporated Research Institute of Seismology (IRIS-DMC) in the epicentral distance ranging

between 30º and 90º. In this distance range, the waveforms are not contaminated by strong upper mantle or core phases. The azimuthal coverage is good enough to resolve some details of the moment release distribution.

Using Quick Epicentre Determination (QED) location and Jeffreys and Bullen (1958) travel time tables, the teleseismic body wave data were appropriately windowed for one minute starting 10s before P-wave arrival or S-wave arrival. The information contained in this time window is adequate enough to resolve the source parameters. The displacements records of P waves as well as SH waves are shown in Figs. 5-6, while station parameters are given in tables 1-2.
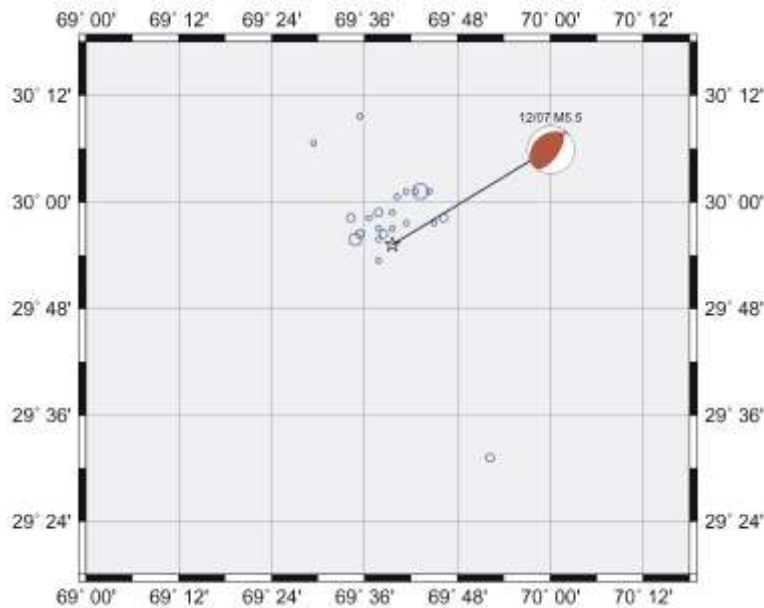

Fig. 4. Map showing the epicentral location of the Barkhan earthquake of July 12, 1999 and distribution of aftershocks (MSSP Data).

Table 1. List of Station Parameters of Barkhan earthquake of June 26, 1999.

Station	AZM	BK-AZM	Delta	P	1/r	Phase	Weight
ISP	294.3	92.0	33.0	0.079	14.10	P-UD	1.0
FURI	240.1	49.5	35.6	0.078	10.80	P-UD	1.0
TRTE	326.9	115.5	40.6	0.075	9.50	P-UD	1.0
TATO	83.0	71.5	46.1	0.125	8.70	SH	0.2
KEV	341.2	126.2	46.4	0.071	8.70	P-UD	1.0
KONO	324.9	99.4	49.3	0.070	8.50	P-UD	1.0
KONO	324.9	99.4	49.3	0.121	8.50	SH	0.2
TIXI	20.1	109.2	52.2	0.118	8.20	SH	0.2
MAHO	299.5	79.2	53.1	0.114	8.00	SH	0.2

WBK-AZM = Azimuth from station to source, P= Ray Parameter (P=Sin i/v where i=angle of incidence), 1/r = Geometrical factor (x1/10 km), Weight = Station weighting factor

Table 2.   List of Station Parameters of Barkhan Earthquake July 12, 1999.

Station Code	AZM	BK-AZM	Delta	P	1/r	Phase	Weight
CHTO	106.0	61.5	29.0	0.081	20.10	P-UD	1.0
CHTO	106.0	61.5	29.0	0.140	20.10	SH	1.0
EIL	277.9	80.3	30.0	0.081	19.10	P-UD	2.0
CSS	288.8	88.9	30.7	0.018	17.40	P-UD	2.0
OBN	326.5	123.4	34.3	0.078	12.20	P-UD	2.0
FURI	240.1	49.4	35.7	0.077	10.80	P-UD	2.0
BJT	59.0	92.3	39.1	0.074	9.80	P-UD	1.0
TRTE	326.8	115.4	40.6	0.074	9.50	P-UD	1.0
MDJ	55.2	85.9	48.9	0.069	8.50	P-UD	1.0
KONO	324.8	99.3	49.3	0.068	8.50	P-UD	2.0
KBS	348.5	116.2	54.5	0.066	8.00	P-UD	2.0
DAV	101.7	58.7	57.3	0.063	7.80	P-UD	2.0
PAB	300.9	74.4	59.7	0.062	7.60	P-UD	2.0
MTE	302.6	73.2	61.8	0.060	7.00	P-UD	2.0

BK-AZM = Azimuth from station to source, P= Ray Parameter (P=Sin i/v where i=angle of incidence), 1/r = Geometrical factor (x1/10 km), Weight = Station weighting factor

Table 3. Near source structure used in the waveform inversion.

V_P	V_S	ρ	D
5.57	3.36	2.65	15
6.50	3.74	2.87	33
8.10	4.68	3.30	-

V_P, V_S = P-wave and S-wave velocities (km/s); ρ = density (10^3 kg/m^3); D = thickness (km)
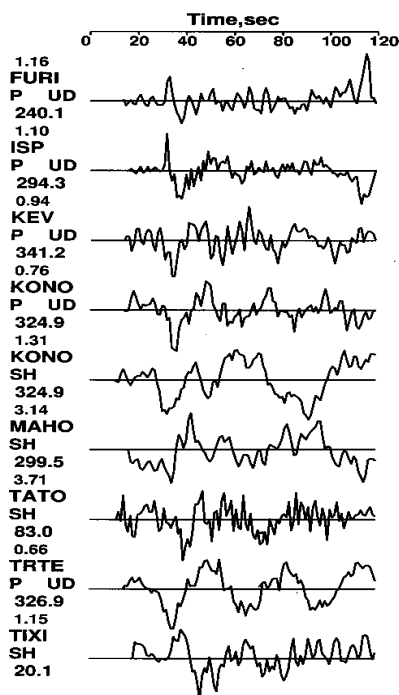

Fig. 5. Body wave recorded by some IRIS stations for the Barkhan Earthquake of June 26, 1999.

3.   Teleseismic body wave inversion

An iterative deconvolution inversion method developed by Kikuchi and Kanamori (1986; 1991) for teleseismic data was employed to resolve the source complexity by matching the waveforms and extraction of the source parameters. First, with the approximations of a single point source, we determined the fault mechanism so that synthetic waveforms are best fit with the observed ones. For the synthetic waveform, we used a three layer structures (two layers of crust and a semi-infinite mantle) in the source region as given in Table 3. As a first step towards the inversion, the Green's function for the six elements of the moment tensor was calculated at different depths beneath the epicenter, assuming a single point source. The focal depth lies within this depth range. In order to get a more realistic waveform, we have to consider the effects of inhomogenity in structure, attenuation during traveling and instruments response. For intrinsic attenuation (Q), the Futterman (1962) operator t* (ratio of travel time to average Q) of 1s was used for P

waves and 4s for S waves (Helmberger, 1983). This Q filter was convolved with a triangular source time function having rise time τ_1 of 2s, source duration τ_2 of 10s and the seismic moment of the order of 10^{18} Nm for June 26, 1999 earthquake and a rise time τ_1 of 4s, source duration τ_2 of 6s and the seismic moment of the order of 10^{18} Nm for July 12, 1999 earthquake. Consequently the seismograms were simultaneously inverted to double couple single point source in the least square sense for the source model parameter, assuming no change in the mechanism during rupture. The inversion process was carried over different depths. The depth yielding the minimum residual was taken as the depth of the source.

For these events a point source model provides more or less equal fits to most of the waveforms. This means that a single source is sufficient to describe the source processes of these earthquakes. The P waves as well as the SH waves records, at different stations (Figs. 5-6) also reflect a smooth rupture. The fit of data i.e. synthetic and observed waveforms for the point source model are shown in Figs. 7-8. Considering the azimuthal coverage and the quality of the observed records, we applied station-weighting factors to both the observed and synthetic waves. The final residual waveform error of June 26, 1999 earthquake is 0.5416 and the best matching double couple with a strike of 243º, a dip of 39º and a rake of 92º shows thrust mechanism with small strike slip component. Also the final residual waveform error of July 12, 1999

earthquake is 0.6050 and the best matching double couple with a strike of 237º, a dip of 32º and a rake of 111º shows thrust mechanism.

Moreover, inversion was done using these solutions as a fixed mechanism with the result indicating a good fit to the data with a final residual error equal to 0.5410 and 0.6040 respectively. A slight change in the parameters of the fault plane caused an increase in the residual error. The final parameters of these solutions are summarized in Table 4.

4. Stress drop and dislocation

Assuming the bilateral rupture propagation, the fault area of this event can be estimated using the relation of Fukao and Kikuchi (1987).
$$S = \pi (V\tau_2 / 2)^2$$
Where V is the rupture velocity and τ represents the rupture duration. Rupture velocity is taken as V=2.5 km/sec. After estimating the aftershock area S, we obtained the average stress drop ($\Delta\sigma$) following Fukao and Kikuchi (1987) as

$(\Delta\sigma) = 2.5\, M_o / S^{3/2}$ (where M_o is the seismic moment)

The stress drop corresponding to these events are 26 bars and 7 bars respectively. According to the slip dislocation theory of faulting (Aki, 1966) the average dislocation (D) can be estimated from

$D = M_o / \mu S$ (where μ is the rigidity: 3×10^{10} N/m^2)

The displacement from the above relation is estimated dislocation as D = 0.031m for June 26 earthquake and 0.023m for July 12 earthquake.

Table 4. Final Source Parameters.

EVENT	Φ	δ	Λ	H	M_o	M_w	$\Delta\sigma$	τ_1	τ_2
June 26, 1999	243	39	92	5.5	2.3×10^{17}	5.5	0.031	2.0	10.0
July 12, 1999	237	32	111	5.0	3.3×10^{17}	5.5	0.023	4.0	6.0

Where Φ = Strike; δ = Dip; λ = Slip; M_o = Seismic Moment; M_w = Moment Magnitude; $\Delta\sigma$ = Stress Drop; τ_1 = Rise Time; τ_2 = Source Duration
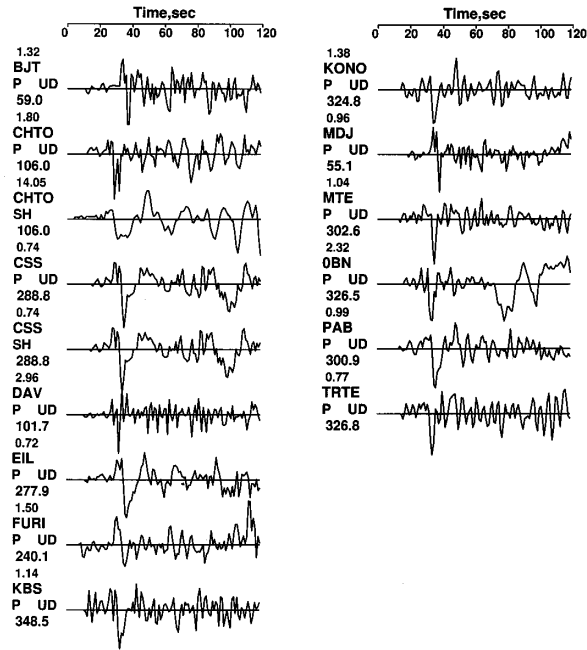
Fig. 6. Body wave recorded by some IRIS stations for the Barkhan earthquake of July 12, 1999.
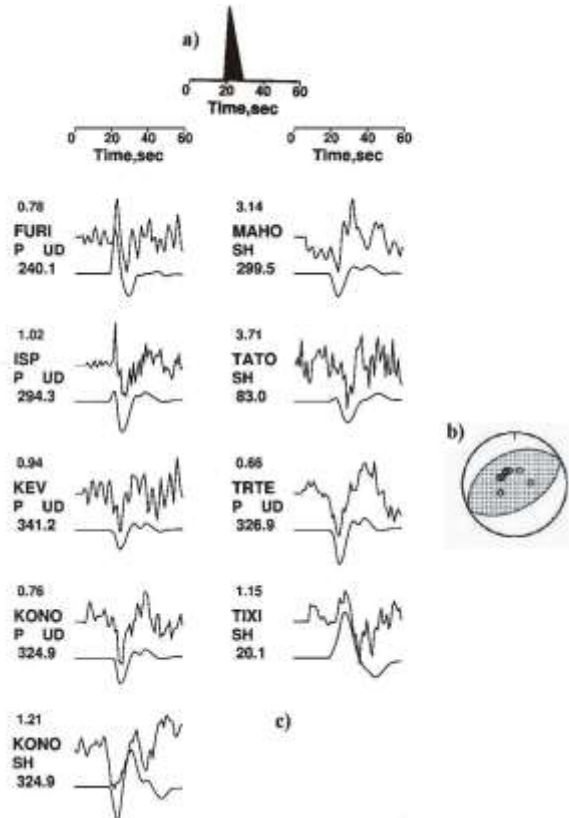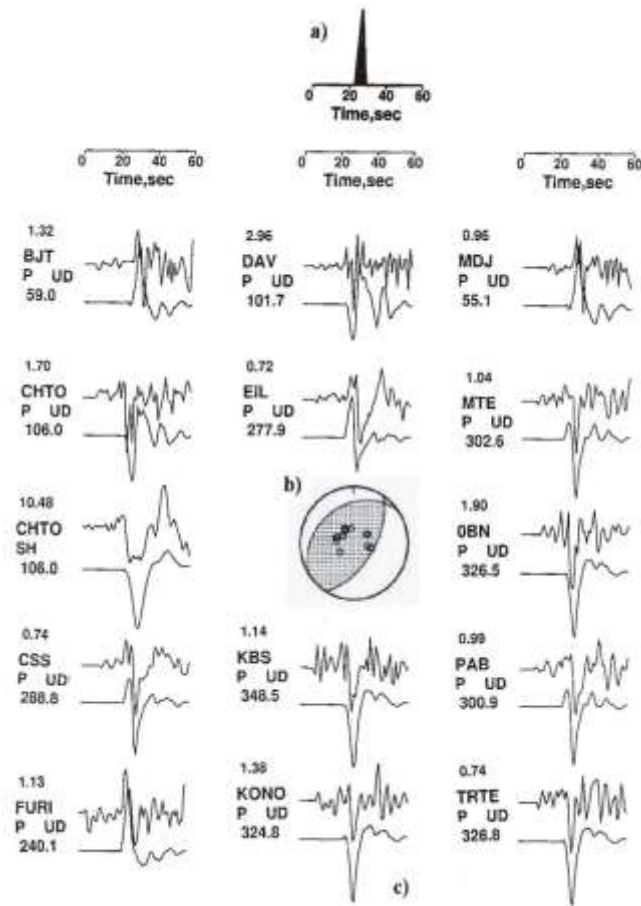

Fig. 7. Barkhan earthquake of June 26, 1999. Results of the inversion of the double couple source, a) seismic moment release as function of time, b) mechanism diagram of the best fit double couple point source, c) observed and synthetic P and SH waveforms. The number in the upper and lower left indicate peak to peak attitude in the microns of the observed records and the azimuth respectively.

Fig. 8. Barkhan earthquake of July 12, 1999: Results of the inversion of the double couple source, a) seismic moment release as function of time, b) mechanism diagram of the best fit double couple point source, c) observed and synthetic P and SH waveforms. The number in the upper and lower left indicate peak to peak attitude in the microns of the observed records and the azimuth respectively.
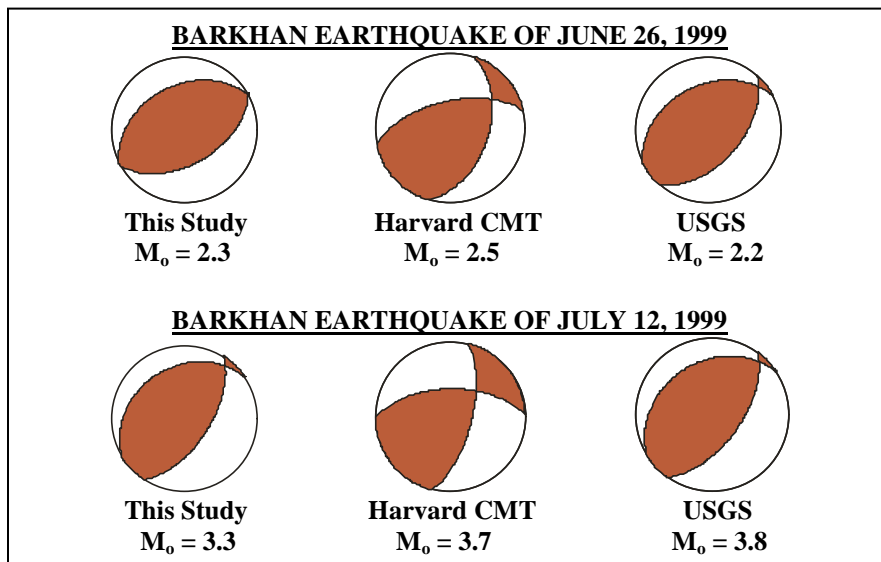

Fig. 9. Mechanism diagram of the total moment tensor for the Barkhan earthquakes of June 26 and July 12, 199 compared with the solution obtained by Harvard CMT and USGS. The seismic moment is given in units of 1017 Nm.

104

5. Results and discussions

Modeling of body waves recorded at teleseismic distances has shown that the fault causing these earthquakes has a thrust mechanism with small strike slip component on a roughly northeast-southwest trend (Figs. 7-9). These earthquakes had a shallow crustal focal depth of 5 km. The cluster of aftershocks indicates nearly the same fault length with unilateral northeast rupture propagation. Waveform analysis and aftershock distribution reveal that these earthquakes represents thrust faulting on a fault with a strike of 243°, a dip of 39°, and a rake of 92° of June 26, 1999 and a strike of 237°, a dip of 32°, and a rake of 111° of July 12,1999. This solution is in agreement with other solutions obtained by other agencies (e.g., USGS, HARVARD). All these solutions indicate predominantly thrust mechanism. The mechanism diagram for the total moment release is shown in Fig. 9. The moment rate function and its area that gives the total seismic moment $M_o = 3.3 \times 10^{17}$ Nm and $M_o = 2.3 \times 10^{17}$ Nm, respectively are shown in Figures 7(a) and 8(a). A comparison between observed and the generated synthetic waveforms at all stations is shown in Figs. 7(c) and 8(c). This seismic moment corresponds to a moment magnitude of 5.5. The stress drop associated with a fault area of 42 km^2 is equal to 26 bars and 7 bars, respectively. The earthquakes and its aftershocks under study seem to lie on the eastern parts of the Karmari and Barkhan thrusts. The aftershocks distribution indicates a northeast-southwest trending rupture plane, which coincides with the eastern section of the Karmari thrust. Both these events investigated here occurred in the upper crust with shallow depth.

Acknowledgements

References

Abdul-Gawad, M., 1971. Wrench movement in the Balochistan and relation to Himalayan-Indian Ocean Tectonics. Bulletin Geological Society of America, 82, 1235-1250.

Aki, K., 1966. Generation and propagation of G waves from the Niigata earthquake at June 16, 1964. Bulletin Earthquake Research Institute, Tokyo University, 44, 73-88.

Bannert D., Cheema A., Ahmed, A., Schaffer, U., 1992. The Geology of the Western Fold Belt: Structural Interpretation of LANDSAT-MSS Satellite Imagery, Pakistan (1:500,000). Federal Institute of Geosciences and Natural Resources (BGR), Hannover, Germany.

Bender, F.K., Raza H. A., 1995. Geology of Pakistan. Gebruder Borntraeger, Berlin-Stuttgart, Germany.

Fukao, Y., Kikuchi, M., 1987. Source retrieval for mantle earthquakes by iterative deconvolution of long period P-waves. Tectonophysics, 144, 249-269.

Futterman, W.I., 1962. Dispersive body wave. Journal of Geophysical Research, 67, 5279-5291.

Helmberger, D.V., 1983. Theory and application of synthetic seismograms, in Earthquakes: Observation, Theory and Interpretation. Societa Italiana di Fisica, Bologna, Italy, 174-222.

Jeffreys, H., Bullen K.H., 1940. Seismological Tables, British Association for the Advancement of Science, London.

Kikuchi, M., Kanamori, H., 1986. Inversion of complex body waves-II. Physics of the Earth and Planetary Interiors, 43, 205-222.

Kikuchi, M., Kanamori, H., 1991. Inversion of complex body waves-III. Bulletin Seismological Society of America, 79, 670-689.

Lawrence, R. D., Khan, S. H., DeJong, K. A., Farah, A., Yeats, R.S., 1981. Thrust and strike-slip fault interaction along the Chaman fault zone, Pakistan. In: McClay, K. R., Price, N. J. (Eds.), Thrust and Nappe Tectonics. Geological Society of London, Special Publication, 9, 363-370.

Lee, W.H.K., 1990. HYPO71PC Programme, IASPEI Software Library, 1.

Sarwar, G., DeJong, K. A., 1979. Arcs, oroclines, syntaxes: The curvature of mountain belts in Pakistan. In: Farah, A., DeJong, K.A. (Eds.), Geodynamics of Pakistan. Geological Survey of Pakistan, 351-358.